Chemical Engineering Journal 157 (2010) 339–347

Contents lists available at ScienceDirect

Chemical Engineering Journal

journal homepage: www.elsevier.com/locate/cej

Activated carbon load equalization of transient concentrations of gas-phase toluene: Effect of gas flow rate during pollutant non-loading intervals

Marilou M. Nabatilan[a], Ameziane Harhad[b], Peter R. Wolenski[b], William M. Moe[a,*]

[a] 3513B Patrick Taylor Hall, Department of Civil and Environmental Engineering, Louisiana State University, Baton Rouge, LA 70803, USA
[b] 304 Lockett Hall, Department of Mathematics, Louisiana State University, Baton Rouge, LA 70803, USA

ARTICLE INFO

Article history:
Received 24 July 2009
Received in revised form 4 November 2009
Accepted 7 November 2009

Keywords:
Attenuation
Biofilter
Dampen
Equalization
GAC
Flow rate
Toluene
Unsteady-state

ABSTRACT

Dynamically varying contaminant concentrations pose a challenge in the design and operation of biofilters for air pollution control. One strategy for managing this problem involves installation of a column packed with granular activated carbon (GAC) to achieve load equalization prior to biofilter treatment. Research described here was conducted to evaluate the effect of changes in gas flow rates during contaminant non-loading intervals on the GAC load equalization process. Toluene served as the model pollutant, and BPL 4 × 6 mesh GAC served as the model adsorbent. Fixed-bed adsorption/desorption experiments were conducted with influent toluene concentrations of 250 ppm_v (superficial gas velocity 300 m/h) for durations of 12, 8, and 4 h/day, and no toluene in the influent air for the remainder of the day to simulate processes with varying work schedules. During toluene non-loading intervals, experiments were conducted with gas flow rates 1.0, 0.50, and 0.10 times the flow rate during toluene loading intervals. Numerical simulations performed using a pore and surface diffusion model, adapted to account for changes in gas flow rate, were in close agreement with experimental measurements. Collectively, experimental data and model simulations demonstrated that relatively small GAC columns (empty bed contact times on the order of a few seconds) can achieve considerable load equalization even when gas flow rates are reduced during contaminant non-loading intervals. Results suggest that in cases where the fraction of time pollutants present in the gas stream are relatively small, use of a passively operated GAC load equalization process in conjunction with reduction in gas flow rates during contaminant non-loading intervals may prove especially attractive.

1. Introduction

Many industrial processes generate off-gases that contain volatile organic compounds (VOCs) that must be treated to meet regulatory requirements and protect public health. Biofilters (fixed-film bioreactors that make use of microorganisms to oxidize VOCs) are an attractive air pollution control option for many contaminated gas streams because of their comparatively low energy requirements and low carbon emissions in comparison to thermal treatment technologies when treating dilute VOC concentrations [1]. While there have been many effective applications of biofilters, fluctuating pollutant concentrations pose a challenge in design and operation. Temporary periods of high influent contaminant concentrations can result in diminished treatment performance because of limitations in biological reaction capacity and mass transfer rates [2–11]. Likewise, transient periods of low or zero contaminant loading can impose starvation conditions on the microbial communities present in a biofilter, resulting in a period of diminished contaminant removal efficiency when pollutant loading resumes [12–16]. Transient loading conditions can also lengthen the time required for biofilter startup [17,18].

One approach for overcoming these challenges is to employ an integrated system comprised of a passively operated load equalization device consisting of a column packed with granular activated carbon (GAC) located in series prior to the biofilter [8,19]. The rationale for such a system is that during periods of high influent contaminant concentration, the GAC adsorbent can temporarily accumulate contaminants and then subsequently desorb contaminants during intervals when concentration in the waste gas is lower. This can decrease peak contaminant loading to biofilters subjected to transient conditions, prevent starvation conditions during periods when influent contaminant concentrations are low or absent, and provide a means of incorporating a safety factor in system design [8,19–22].

Previous studies on passively operated GAC load equalization systems, however, have been limited to cases with constant gas flow rates during pollutant loading and non-loading intervals. While it is generally recommended that sufficient airflow should

---

* Corresponding author. Tel.: +1 225 578 9174; fax: +1 225 578 8652.
E-mail address: moemwil@lsu.edu (W.M. Moe).

1385-8947/$ – see front matter © 2009 Elsevier B.V. All rights reserved.
doi:10.1016/j.cej.2009.11.012

Nomenclature

$C_{0,i}$	initial influent concentration (M/L^3)
$C_i(z,t)$	adsorbent concentration in bulk phase (M/L^3)
$C_{p,i}(r,z,t)$	adsorbate concentration in adsorbent pores (M/L^3)
$D_{p,i}$	pore diffusivity (L^2/T)
$D_{s,i}$	surface diffusivity (L^2/T)
$k_{f,i}$	film transfer coefficient (L/T)
L	bed length (L)
m	number of components
$q_i(r,z,t)$	adsorbent phase concentration (M/M)
R	average adsorbent particle radius (L)
V	loading rate (L/T)
Greek letters	
ε_P	particle void fraction (porosity)
ρ_A	apparent adsorbent density (M/L^3)
ε	bed void fraction
subscripts	
i	component number i

be maintained in biofilters even during periods of no contaminant loading to prevent development of anaerobic conditions in the biofilter [1,14], reduction of gas flow rates during intervals when contaminants are not being generated are sometimes used to minimize power costs associated with blower operation. Because costs associated with blower operation often comprise a relatively large fraction of biofilter operating costs [1], this can have a large influence on total operating costs.

The objective of research reported here was to characterize GAC load equalization performance in cases where gas flow rates are decreased during intervals of no contaminant loading. A series of fixed-bed sorption experiments was conducted, with intermittent loading of toluene and time varying air flow rate. During contaminant non-loading periods, air flow rates were reduced to various fractions (e.g., 0.50, 0.10) of the baseline full flow rate maintained during contaminant loading periods. The durations of contaminant loading tested were 12, 8, and 4 h/day (with associated non-loading intervals of 12, 16, and 20 h/day, respectively). A simple theoretical relationship based on mass balance calculations was developed to determine the maximum GAC column load equalization performance that can be achieved at various loading durations and air flow rate reductions during non-loading intervals. A pore and surface diffusion model adapted to account for changes in gas flow rates as a function of time was used to simulate the load equalization process.

2. Materials and methods

2.1. Experimental testing of GAC load equalization

The experimental apparatus used in fixed-bed adsorption/desorption experiments (supplemental Fig. S1) employed packed columns constructed of 7.62 cm ID PVC pipe. Each contained a stainless steel support mesh at the bottom, 6-cm depth glass beads (5 mm diameter) to distribute air flow, a thin layer of glass wool, a 33.3-cm layer of BPL 4 × 6 mesh GAC (mass 716 g, packed bed volume 1.52 L) (Calgon Carbon Corp., Pittsburgh, PA), another thin layer of glass wool, and another 6-cm glass beads. GAC was rinsed with distilled water to remove fines, dried at 105 °C, and stored in desiccators prior to use.

The system included two air supply lines constructed of Teflon tubing. One provided air flow during periods of toluene loading, and the other provided contaminant-free air flow during periods of no toluene loading. Airflow from each of the supply lines was controlled by a solenoid valve (Asco Valve Inc., NJ), which was turned on and off using a microprocessor-based controller (Chron-Trol, San Diego, CA). Air flow rate in each supply stream was controlled using an electronic mass flow controller (Aalborg Instruments, Orangeburg, NY). During toluene loading intervals, liquid toluene (ACS reagent grade, Sigma, St. Louis, MO) was delivered by syringe pumps (KD Scientific, Boston, MA) and evaporated into the air stream. Initial tests conducted prior to placement of activated carbon demonstrated that components other than GAC had little or no adsorption capacity for toluene. All experiments were conducted at ambient laboratory temperature of $23 \pm 2\,^\circ$C.

Experiments employed three separate columns that were supplied with air containing 250 ppm$_v$ toluene for 12, 8, and 4 h/day, respectively. For all experiments, air flow rate entering the GAC columns during toluene loading intervals was 22.8 L/min, corresponding to superficial gas velocity of 300 m/h in the packed columns. Initially, each column also received air at full flow of 22.8 L/min during toluene non-loading periods. This loading was continued until a consistent pattern of attenuated effluent toluene concentrations was exhibited on a daily basis and daily toluene mass balance closure was >95%. Hereafter, this condition is referred to as quasi-steady-state. After quasi-steady-state was achieved at the initial loading condition, the air flow rate during toluene non-loading periods was sequentially reduced to 0.50 and then 0.10 times full flow (i.e., 11.4 or 2.28 L/min, corresponding to superficial gas velocity of 150 or 30 m/h in the packed columns) while maintaining full flow rate (i.e., 22.8 L/min) during daily toluene loading intervals. For each loading condition tested, the systems were allowed to reach quasi-steady-state, and effluent toluene concentrations were measured for at least 5 days before loading conditions were changed.

2.2. Analytical procedures

Influent and effluent toluene concentrations were measured using a model 1312 photo-acoustic multi-gas monitor (California Analytical, Orange, CA), with concentrations recorded at 1.0 min intervals.

2.3. Mass balance calculations of ideal load equalization

A simple mass balance approach was employed to calculate the “ideal” load equalization that could be achieved by GAC columns subjected to flow rate reductions during periods when no toluene was present in the airflow. “Ideal” load equalization would be observed if the toluene concentration exiting the GAC column were constant as a function of time at a level equal to the flow-weighted average influent concentration (including toluene loading and non-loading intervals). In the mass balance approach, it was assumed that full baseline air flow rate, Q_o, would occur during toluene loading intervals, while a fraction of the baseline airflow would occur during toluene non-loading periods. At quasi-steady-state, the toluene mass entering a GAC column on a daily basis would equal the mass exiting the column on a daily basis (i.e., the net mass adsorbed would equal the net mass desorbed and there would be no net accumulation in the column). The total toluene mass exiting the GAC column on a daily basis includes mass exiting during intervals of full flow (interval when toluene is present in the influent) and intervals of partial flow (when toluene is absent from the influent) as indicated in Eq. (1).

$$C_oQ_ot_o = C_{avg}Q_ot_o + C_{avg}f_QQ_ot_p \qquad (1)$$

where C_o = influent toluene concentration during the loading interval; C_{avg} = the flow-weighted average effluent toluene concentration at quasi-steady-state, assuming perfect load equalization; Q_o = volumetric air flow rate during toluene loading intervals (full flow); f_Q = fraction of the baseline volumetric air flow rate maintained during toluene non-loading intervals (partial flow); t_o = daily duration of toluene loading at full volumetric air flow rate (i.e., at $Q = Q_o$); t_p = daily duration of no toluene loading with air at partial flow (i.e., at $Q = f_Q Q_o$).

Dividing all terms in Eq. (1) by the air flow rate during toluene loading intervals (Q_o) and then rearranging terms results in definition of the ideal load equalization, expressed in terms of dimensionless effluent toluene concentration, as shown in Eq. (2).

$$\frac{C_{avg}}{C_o} = \frac{t_o}{t_o + f_Q t_p} \tag{2}$$

2.4. Pore and surface diffusion model

The pore and surface diffusion model (PSDM) described by Crittenden et al. [23] and Hand et al. [24] was adapted to simulate the dynamic toluene adsorption and desorption on GAC under loading conditions characterized by reduced flow rates during pollutant non-loading intervals. The PSDM is a dynamic fixed-bed model that incorporates several assumptions [25]: (1) plug-flow conditions exist in the bed; (2) linear driving force describes the local bulk phase mass flux at the exterior surface of the adsorbent particle; (3) local adsorption equilibrium exists between the solute adsorbed onto the GAC particle and the solute in the intra-aggregate stagnant fluid; (4) intraparticle mass flux is described by surface and pore diffusion; and (5) adsorption equilibrium of an individual compound can be represented by the Freundlich isotherm equation.

In the PSDM, two partial differential equations (PDEs), obtained for each adsorbing component from mass balances on the bulk gas phase and the adsorbed phase, are coupled together from an assumption of local equilibrium at the exterior of the adsorbent particle. Derivation of these equations for conditions of constant gas flow rate has been presented previously [23,25,26].

The bulk gas phase mass balance for component i (in this case, toluene) is given by Eq. (3) (see Nomenclature section for definition of variables).

$$\frac{\partial C_i}{\partial t}(z,t) + V(t)\frac{\partial C_i}{\partial z}(z,t) + 3\frac{k_{f,i}(1-\varepsilon)}{\varepsilon R}\left[C_i(z,t) - C_{p,i}(r=R,z,t)\right] = 0 \tag{3}$$

This is identical to the equation for the bulk gas phase mass balance presented previously [23,25,26] except that in the equation presented here, the term $V(t)$ describes the intermittent change in velocity brought about by intermittent change in gas flow rate (as opposed to an assumed constant flow rate in the previous work [23,25,26]).

The initial and boundary conditions are respectively:

$$C_i(z,t) = 0 \quad \text{at} \quad 0 \le z \le L,\ t = 0 \tag{4}$$

$$C_i(z,t) = C_{0,i}(t) \quad \text{at} \quad z = 0,\ t > 0 \tag{5}$$

In the adsorbent, the intraparticle phase mass balance for component i in an assumed spherical particle is given by:

$$\frac{1}{r^2}\frac{\partial}{\partial r}\left[r^2 D_{s,i}\frac{\partial q_i}{\partial r}(r,z,t) + \frac{r^2 D_{p,i}\varepsilon_P}{\rho_A}\frac{\partial}{\partial r}C_{p,i}(r,z,t)\right] = \frac{\partial}{\partial t}\left[q_i(r,z,t) + \frac{\varepsilon_P}{\rho_A}C_{p,i}(r,z,t)\right] \tag{6}$$

The initial condition and boundary conditions are, respectively:

$$q_i(r,z,t) + \frac{\varepsilon_P}{\rho_A}C_{p,i}(r,z,t) = 0 \quad \text{at} \quad 0 \le r \le R,\ t = 0 \tag{7}$$

$$\frac{\partial}{\partial r}\left[q_i(r,z,t) + \frac{\varepsilon_P}{\rho_A}C_{p,i}(r,z,t)\right] = 0 \quad \text{at} \quad r = 0,\ t \ge 0 \tag{8}$$

$$D_{s,i}\rho_A\frac{\partial q_i}{\partial r}(r=R,z,t) + D_{p,i}\varepsilon_P\frac{\partial C_{p,i}}{\partial r}(r=R,z,t) = k_{f,i}\left[C_i(t) - C_{p,i}(r=R,z,t)\right] \tag{9}$$

Concentration of component i in the gas phase of GAC pores and in the adsorbent phase of particles are coupled in Eq. (10) with the assumption that the adsorption rate is much faster than the mass transfer rate (assumption of local equilibrium).

$$C_{p,i}(r,z,t) = \frac{q_i(r,z,t)}{\sum_{k=l}^{m} q_k(r,z,t)}\left[\frac{\sum_{k=l}^{m} n_k q_k(r,z,t)}{n_i K_i}\right]^{n_i} \tag{10}$$

To implement the numerical approach in solving the system of PDEs describing the dynamics in a fixed-bed adsorber, a modification of the MATLAB program previously described by Nabatilan et al. [22] was employed. The program used a solution methodology that closely followed the numerical approach presented by Friedman [26] and Crittenden et al. [23]. The PDEs, initial conditions, and boundary conditions were first converted into dimensionless form and then reduced to a system of ordinary differential equations (ODEs) by the method of orthogonal collocation [23,26]. In the present model, some dimensionless parameters (including dimensionless time) are a function of the fluid residence time in the packed bed, which in turn is a function of gas flow rate and velocity; hence, these were intermittently updated throughout the simulation period to account for step changes in flow rates. Additional details regarding dimensionless parameters and calculation methodology are presented as supplementary material (Appendix A).

The resulting system of ODEs was solved using the MATLAB solver ode15s, which is designed for stiff problems. The ode15s subroutine is a variable order solver based on the numerical differentiation formulas (NDFs); optionally, it uses the backward differentiation formulas (also known as Gear's method) that are usually less efficient [27]. During the validation process of the MATLAB code, the effect of the number of collocation points in the axial and the radial directions was investigated by systematically varying the number of collocation points from 5 to 22 and from 3 to 6 in the axial and radial directions, respectively. All of the model simulations presented here were conducted with 18 axial collocation points and 6 radial collocation points, reflecting conditions where an increase in number of collocation points would not have made a difference in the results reported.

Calculations using the PSDM require equilibrium parameters, kinetic parameters, physico-chemical properties of adsorbing compound(s) and adsorbent, gas properties, concentration data, and column dimensions. Parameter values and sources of data input to the model are presented in Supplementary Table S1. Time varying influent air flow rates and influent toluene concentrations input to the model were identical to the target loading conditions that were experimentally tested.

To investigate the effects of GAC packed bed depth on load equalization in systems with decreases in air flow rate during toluene non-loading intervals, the new MATLAB code was used to simulate transient loadings with GAC packed bed depths ranging from 2.0 to 50.0 cm.

3. Results

3.1. GAC column load equalization at various reduced air flow rates during contaminant non-loading periods

Following the start of loading to each of the experimentally tested columns, there was an initial period during which toluene accumulated in the GAC column and no toluene was detected in the effluent (see example in Supplementary Fig. S2). Eventually, breakthrough occurred, and then a consistent pattern of attenuated effluent toluene concentrations was exhibited on a daily basis. Hereafter, this condition is referred to as quasi-steady-state behavior. In the case of 250 ppm$_v$ toluene loading for 12 h/day and uncontaminated air flow at the same rate during contaminant non-loading intervals, appreciable toluene breakthrough was observed after 9 days, and quasi-steady-state was achieved after approximately 14 days of intermittent toluene loading (Supplementary Fig. S2).

Experimental measurements and model simulations of quasi-steady-state toluene concentrations exiting from GAC columns receiving gas flow with 250 ppm$_v$ toluene for daily durations (t_o) of 12, 8, and 4 h/day and uncontaminated air at various flow rates (f_Q = 1.0, 0.50, or 0.10) during toluene non-loading intervals are shown in Fig. 1. Each graph depicts data from a 5-day interval with contaminant concentrations measured at 1-min intervals. Time zero on each plot corresponds to the start of a loading period after quasi-steady-state was achieved. The y-axis of each graph depicts the dimensionless effluent toluene concentration (effluent concentration divided by corresponding target influent concentration entering during the loading interval, C_o = 250 ppm$_v$). Measured influent toluene concentrations were found to closely match target concentrations (within 5% of target values, data not shown). In all columns, experimentally measured maximum and minimum toluene concentrations exiting the GAC columns on a daily basis were consistently reproducible (differing by <3%), and mass balance calculations verified that toluene mass entering and exiting the columns on a daily basis were essentially equal (mass balance closure ≥95%).

Several trends are readily apparent from the experimental measurements depicted in Fig. 1. First, for a given duration of daily toluene loading (t_o), average effluent concentrations observed at quasi-steady-state increased as flow rate during the toluene non-loading period decreased. For example, for the GAC column loaded with toluene for 12 h/day (Fig. 1, column 1), the average dimensionless effluent toluene concentrations increased from 0.50 to 0.67 to 0.88 (corresponding to 125, 168, and 219 ppm$_v$ toluene, respectively), as air flow rate during toluene non-loading intervals decreased from 22.8 to 11.4 to 2.28 L/min, respectively (i.e., for f_Q = 1.0, 0.50, and 0.10, respectively).

Second, for a given flow rate during toluene non-loading intervals (f_QQ_o), a shorter duration of daily toluene loading (t_o) resulted

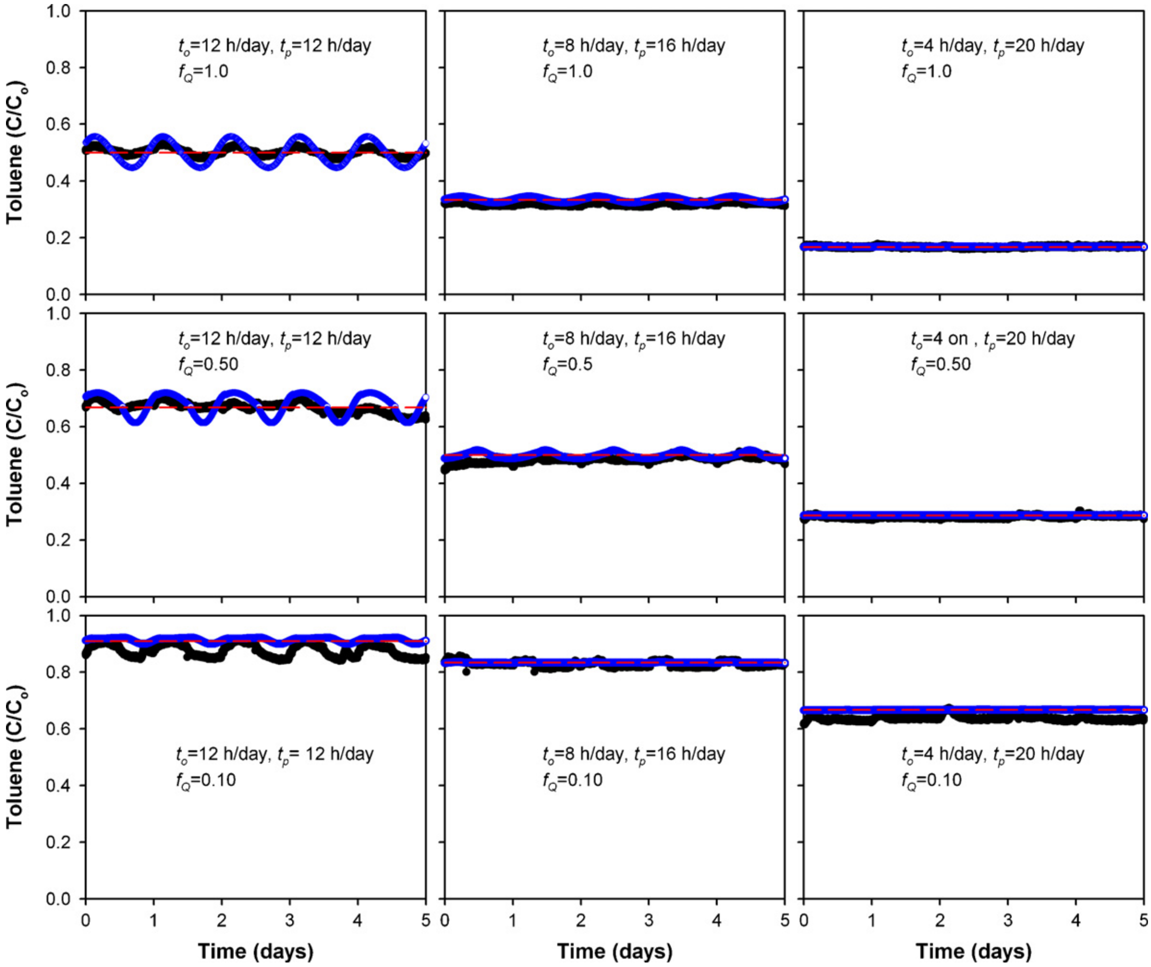

Fig. 1. Experimental measurements (black), PSDM simulations (blue), and "ideal buffering" (red) toluene concentrations exiting GAC columns (33.3 cm packed bed depth) loaded with 250 ppm$_v$ toluene at full flow rate (i.e., 22.8 L/min) during a portion of each day and at various flow rates during toluene non-loading periods. Top: full flow (i.e., f_Q = 1.0, f_QQ_o = 22.8 L/min); middle: 50% of full flow (i.e., f_Q = 0.50, f_QQ_o = 11.4 L/min); bottom: 10% of full flow (i.e., f_Q = 0.10, f_QQ_o = 2.28 L/min). Duration of daily toluene loading period: 12 h/day (left); 8 h/day (middle); 4 h/day (right). (For interpretation of the references to color in the citation of this figure, the reader is referred to the web version of the article.)

in lower average effluent toluene concentrations. For example, when the flow rate during toluene non-loading intervals was half of that during the toluene loading interval (i.e., $f_Q = 0.50$), the dimensionless average effluent toluene concentrations (±standard deviations) determined over 5 days of monitoring at quasi-steady-state were 0.67 ± 0.01, 0.48 ± 0.01, and 0.28 ± 0.002 for loading durations of 12, 8, and 4 h/day, respectively (Fig. 1, row 2). At the same time, variation between daily minima and maxima also decreased as duration of the daily toluene loading interval decreased. For the shortest duration of loading tested here (i.e., $t_o = 4$ h/day), effluent toluene profiles were almost straight lines with little variation between daily maximum and minimum concentrations; hence, the highest degree of load equalization for the same f_Q. This is consistent with the previous finding that an increase in load equalization occurred when the fraction of time during which toluene was supplied to GAC columns decreased when gas flow rates during toluene non-loading intervals were the same [21].

PSDM simulations were in close agreement with experimental measurements. Differences between measured and modeled maximum daily effluent concentrations were consistently small, averaging 3.6 ppm$_v$ ($C/C_o = 0.014$). Discrepancies were largest for the case of 12 h/day toluene loading and no decrease in flow rate during toluene non-loading intervals (i.e., $f_Q = 1.0$), but the difference was relatively small, 7.4 ppm$_v$ ($C/C_o = 0.030$). Similarly, the difference between measured and modeled minimum daily effluent concentrations were also consistently small, averaging 7.1 ppm$_v$ ($C/C_o = 0.028$) with largest discrepancy of 14.2 ppm$_v$ ($C/C_o = 0.056$) in the case of 12 h/day toluene loading with flow rate of 2.28 L/min during toluene non-loading intervals (i.e., $f_Q = 0.10$).

As further described in Section 3.2 below, the toluene concentrations exiting the GAC columns in all of the loading scenarios tested here were close to the concentrations expected from "ideal" load equalization (see dashed lines in Fig. 1).

3.2. "Ideal" load equalization in columns with flow rate reduction during contaminant non-loading periods

Dimensionless effluent toluene concentrations expected for ideal load equalization conditions, as calculated by Eq. (2) for loading scenarios comprised of various durations of daily toluene loading (t_o) and various fractions of air flow rate turn-down (f_Q) during toluene non-loading intervals, are shown in Fig. 2. As shown in the figure, mass balance calculations demonstrate that toluene concentrations exiting a GAC column load equalization device once quasi-steady-state conditions are achieved have an upper limit that approaches the influent concentration (i.e., $C/C_o = 1.0$) as the fraction of air flow during the toluene non-loading interval (f_Q) approaches zero. This results from the fact that as the volume of clean air passing through a GAC column decreases, there is less air volume for toluene temporarily accumulated in the column to be distributed into. If the air flow rate during toluene non-loading intervals was zero, in the absence of net accumulation in the GAC column (a necessary condition for quasi-steady-state), the effluent toluene concentration would equal the toluene concentration entering during the loading interval. Alternately, if the flow rate during the toluene non-loading rate is greater than zero, then the mass of toluene exiting the column is diluted into a larger volume of air, resulting in a lower average effluent toluene concentration. At $f_Q = 1.0$ (the case of constant air flow during loading and non-loading intervals) and constant pollutant concentration during loading intervals, ideal load equalization results in a dimensionless effluent pollutant concentration equal to the fraction of time pollutants are present in the influent (see Eq. (2)). For pollutant loading durations of 12, 8, and 4 h/day as was experimentally tested here, this corresponds to dimensionless effluent concentrations of 0.50, 0.33, and 0.17, respectively.

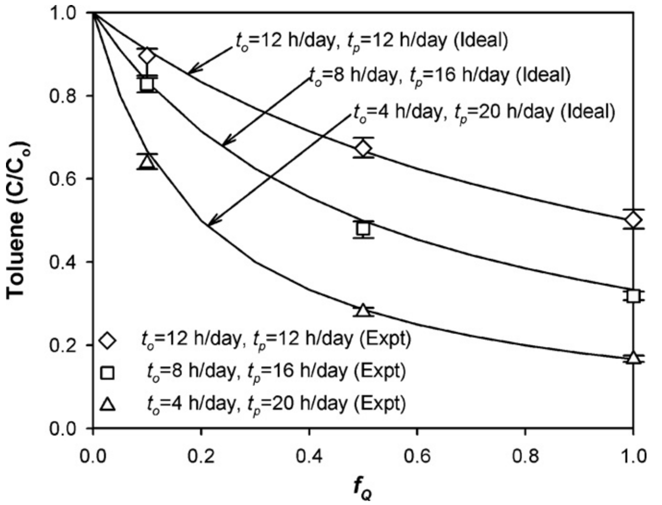

Fig. 2. "Ideal" GAC column load equalization (lines) and experimental measurements (symbols) at quasi-steady-state for various daily durations ($t_o = 12$, 8, or 4 h/day) of 250 ppm$_v$ toluene loading and various airflow rates during toluene non-loading periods (expressed in terms of f_Q, the fraction of the baseline gas flow rate maintained during toluene non-loading intervals). Data points represent average concentrations determined from 5 days of experimental measurements in 33.3 cm packed bed depth columns. Upper bars represent the average daily maxima, and lower bars represent the average daily minima measured at quasi-steady-state.

Experimentally measured data from 33.3 cm packed bed depth GAC columns are depicted in Fig. 2 as symbols. Each data point represents the average toluene concentration exiting the GAC column during 5 days of monitoring at quasi-steady-state. Upper and lower bars represent the average dimensionless maximum (C_{max}/C_o) and minimum (C_{min}/C_o) daily effluent toluene concentrations, respectively. As shown, the experimental data were in close agreement with the ideal load equalization levels. This demonstrates that comparatively small columns (packed bed depth 33.3 cm, EBCT of 4.0 s during full flow conditions) can achieve close to the maximum theoretical degree of load equalization.

3.3. Model simulation of GAC column performance at various column heights

To further explore the range of load equalization behavior expected from GAC columns subjected to intermittent loading conditions combined with gas flow rate reduction during contaminant non-loading intervals, additional model simulations were performed for the loading conditions that were experimentally tested but for a variety of longer and shorter GAC bed depths (ranging from 2 to 50 cm). Input parameters, other than column dimensions and GAC mass used in simulations, were identical to those corresponding to experimental tests.

To represent the data in a form amenable to direct use as a tool for design or analysis, C_{max}/C_o and C_{min}/C_o were plotted as a function of bed depth (Fig. 3). Similar to what was reported previously for cases of constant air flow rate [20–22], toluene was more attenuated (i.e., characterized by lower C_{max}/C_o and higher C_{min}/C_o) as bed depth increased, asymptotically approaching "ideal" buffering for all of the loading conditions analyzed here. Simulation results demonstrate that the packed bed depth necessary to approach the ideal buffering level decreases as the fraction of time for toluene loading decreases. Consistent with the near constant effluent toluene concentration profiles experimentally observed for cases of toluene loading 4 h/day (Fig. 1, last column), simulation results indicate that GAC columns having less than half of the experimentally tested packed bed depth of 33.3 cm would have been sufficient to achieve near ideal load equalization of

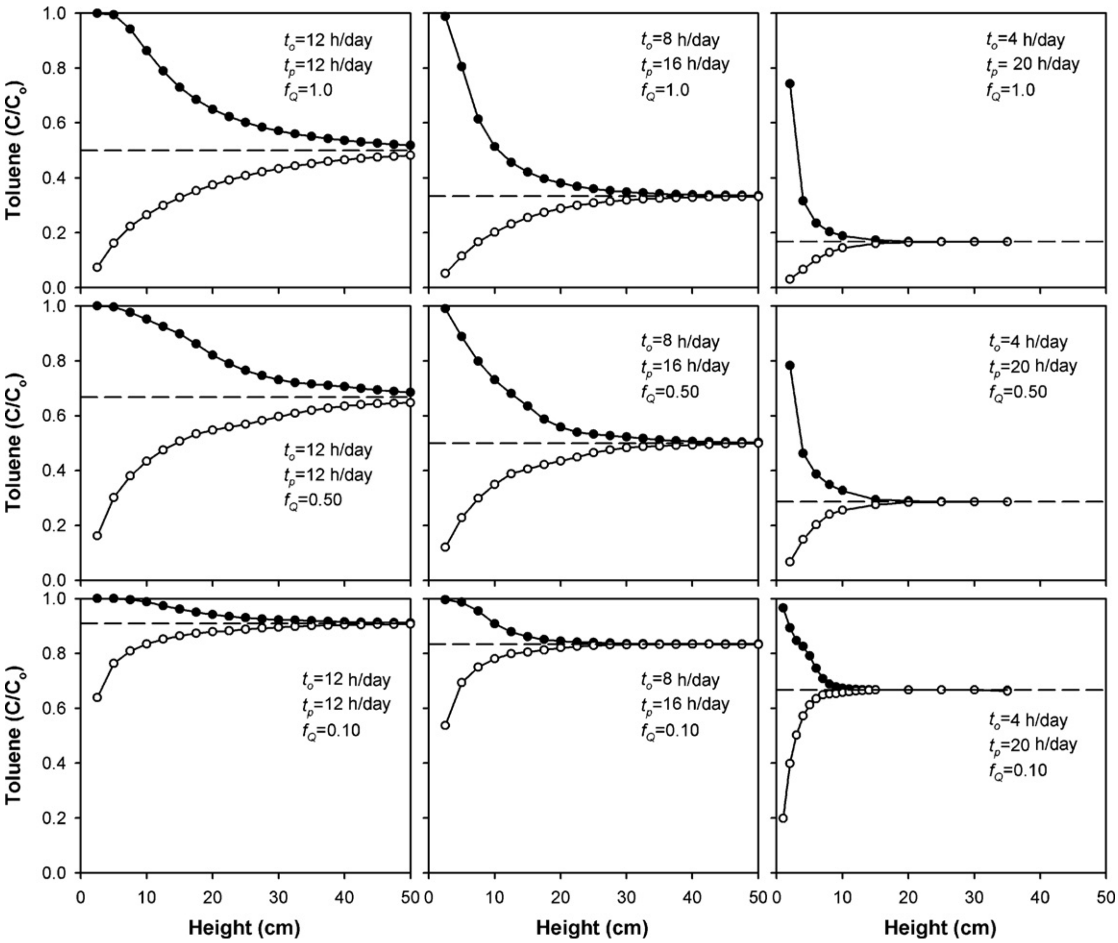

Fig. 3. PSDM simulation results for maximum (filled symbols) and minimum (open symbols) daily dimensionless effluent toluene concentrations as a function of packed bed depth at quasi-steady-state for influent toluene concentration of 250 ppm$_v$ for 12 h/day (left), 8 h/day (middle), and 4 h/day (right) with various gas flow rates during toluene non-loading intervals (f_Q ranging from 1.0 (top) to 0.10 (bottom). Dashed lines denote ideal buffering levels.

toluene at all three air flow rates tested (f_Q = 1.0, 0.50, or 1.0) during toluene non-loading intervals (Fig. 3, last column). For cases with toluene present for a longer duration per day (i.e., 12 or 8 h/day), the GAC bed depth required to approach ideal load equalization was longer (Fig. 3, first two columns).

3.4. Toluene mass fluxes

Consistent with the fact that toluene concentrations exiting the GAC columns (Fig. 1) were relatively constant with time, toluene mass fluxes exiting the GAC columns were relatively constant with time when there was no change in flow rate (i.e., f_Q = 1.0) during pollutant non-loading intervals (Fig. 4, row 1). When the airflow rate during pollutant non-loading intervals was reduced to 0.50 or 0.10 times the flow rate provided during toluene loading intervals, however, toluene mass fluxes varied considerably (Fig. 4, rows 2–3). Maximum mass fluxes were observed during toluene loading intervals (full flow rate) while minimum fluxes were observed during intervals of toluene non-loading when air flow rate was reduced to a fraction of the full air flow. For a given daily duration of toluene loading (t_o), higher daily maximum mass fluxes and lower daily minimum mass fluxes were observed as the flow rate during toluene non-loading intervals decreased. For example, when the column received toluene loading 4 h/day, daily maximum toluene mass fluxes averaged over 5 days of quasi-steady-state increased from 49.7 g/m^2 h (grams toluene per m^2 GAC bed cross-sectional area per hour) to 82.9 and 187 g/m^2 h when flow rate during the 20 h/day interval of toluene non-loading was reduced from 1.0 to 0.50 and 0.10 times full flow rate. For a given reduction in flow rate during the daily pollutant non-loading interval (i.e., fixed f_Q), toluene mass flux rates decreased with decreasing duration of daily pollutant loading. For example, when flow rates during pollutant non-loading intervals were reduced by half (i.e., f_Q = 0.50), average maximum daily toluene fluxes were 197, 142, and 82.9 g/m^2 h for daily toluene loading durations of 12, 8, and 4 h/day, respectively.

For illustrative purposes, dimensionless maximum ($N_{\max}/N_o$) and minimum ($N_{\min}/N_o$) daily toluene mass fluxes corresponding to ideal load equalization levels were calculated for various durations of daily pollutant loading (t_o = 12, 8, or 4 h/day) and various flow rate reductions during pollutant non-loading intervals (f_Q = 0–1.0) based on Eq. (2) and the column geometry and target loading rates employed in the experimental testing (Fig. 5). Mass fluxes are expressed in dimensionless form as the ratio of the maximum or minimum flux exiting the GAC column to the flux entering during toluene loading intervals (N_o). Fluxes calculated from experimental measurements in 33.3 cm bed depth columns loaded with 250 ppm$_v$ toluene are depicted as symbols with error bars representing standard deviation. Due to the high consistency in experimental data, most of the error bars are obscured by symbols in the graphs.

As depicted in Fig. 5, maximum mass fluxes have an upper limit that approaches the level during loading period (i.e., $N_{\max}/N_o$ = 1.0) as flow rate during the pollutant non-loading interval approaches zero. Minimum fluxes, on the other hand, have a lower limit that approaches zero. For a given duration of daily toluene loading (t_o), at quasi-steady-state and ideal GAC buffering, maximum and

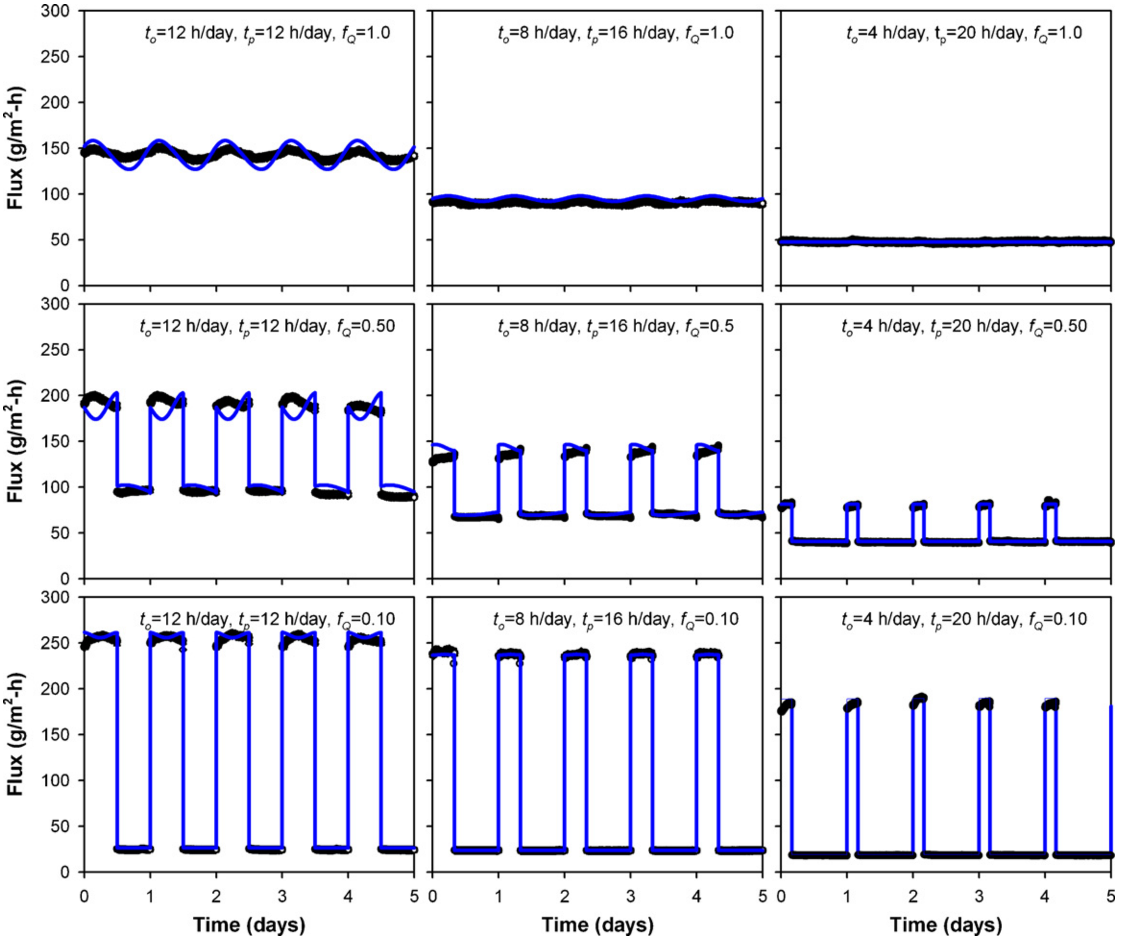

Fig. 4. Quasi-steady-state toluene mass fluxes exiting GAC columns (33.3 cm packed bed depth) loaded with 250 ppm$_v$ toluene at full flow rate (i.e., 22.8 L/min) during a portion of each day and at various flow rates during toluene non-loading periods. Experimental values: black lines; model simulations: blue lines. top: full flow (i.e., f_Q = 1.0, $f_Q Q_o$ = 22.8 L/min); middle: 50% of full flow (i.e., f_Q = 0.50, $f_Q Q_o$ = 11.4 L/min); bottom: 10% of full flow (i.e., f_Q = 0.10, $f_Q Q_o$ = 2.28 L/min). Duration of daily toluene loading period (t_o): 12 h/day (left); 8 h/day (middle); 4 h/day (right). (For interpretation of the references to color in the citation of this figure, the reader is referred to the web version of the article.)

minimum fluxes converge to a common level when the air flow rate during pollutant non-loading intervals is equal to the flow rate during pollutant loading intervals (i.e., f_Q = 1.0). As shown, experimental measurements from 33.3 cm packed bed columns were quite close to the ideal levels.

4. Discussion

Data presented in Fig. 1 support the previously reported finding [19–22] that toluene mass can be temporarily accumulated in a GAC column during intervals when influent concentrations are high and then desorb within a sufficiently short time interval (i.e., during each loading cycle when influent contaminant concentrations are low or zero) to be of practical benefit as a passively operated load dampening equalization mechanism even with intermittently varied air flow rates. The only driving force necessary for toluene desorption was the decrease in influent contaminant concentration imposed by the gas stream. Regeneration of the GAC through other means (e.g., heating, pressure swing [11,28]) was not necessary.

Comparison of dynamic model simulations with experimental measurements (Fig. 1) revealed a good qualitative and quantitative fit for quasi-steady-state breakthrough curves. In fact, in many cases the symbols denoting model simulations are obscured by the experimentally measured data points because of the close fit, particularly for the 4 h/day toluene loading scenario. At the longest daily duration of toluene loading (i.e., 12 h/day), the model consistently over-predicted the maximum effluent toluene concentrations exiting the GAC columns, but by a relatively small amount. Considering the fact that all model simulations reported herein were conducted exclusively using parameter values reported in the literature without any additional calibration, the predictive capability of the model is impressive. This provides further validation that the PSDM is able to well describe the process of load equalization in GAC columns receiving intermittent loading of toluene vapors as reported previously [20–22]. The approach for extending the model to allow simulation of dynamic loading condition characterized by time varying air flow rates in addition to time varying influent pollutant concentrations may prove useful in analysis of systems subjected to a wide variety of unsteady loading conditions.

As shown in Figs. 1 and 2, toluene was well buffered near the ideal level at all of the experimentally tested loading conditions, demonstrating that close to the maximum theoretical level of load equalization (Eq. (2)) can be achieved by GAC columns with EBCTs that are small compared to the EBCTs typical of biofilters (which are typically on the order of 30–60 s [1]). Inspection of model-generated curves shown in Fig. 3 indicates that GAC bed depths substantially smaller than the experimentally tested columns could have achieved roughly the same degree of load equalization for many of the loading scenarios, especially with 4 h/day toluene loading.

While toluene concentrations exiting the GAC columns subjected to daily flow rate reductions during pollutant non-loading

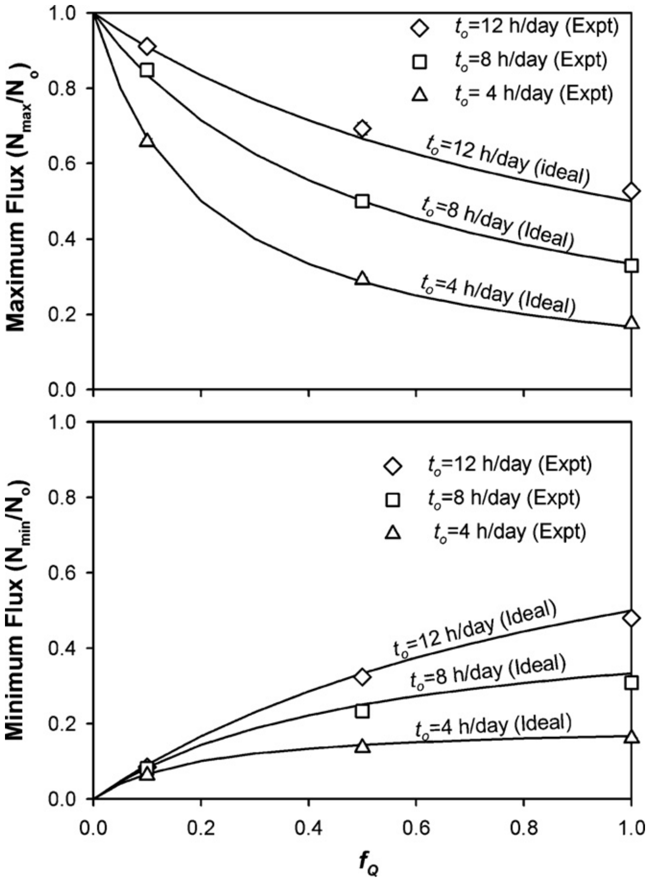

Fig. 5. Maximum (top) and minimum (bottom) dimensionless toluene mass fluxes at quasi-steady-state for various daily durations (t_o = 12, 8, or 4 h/day) of 250 ppm$_v$ toluene loading and various decreased airflow rates (f_Q = 0–1.0) during daily toluene non-loading periods (t_p = 12, 16, and 20 h/day). Lines represent mass fluxes during ideal load equalization. Symbols represent averages determined from at least 5 days of experimental measurements in columns with GAC packed bed depth of 33.3 cm.

intervals were relatively constant with time, toluene mass fluxes exiting the columns dynamically varied with changes in gas flow rate. Maximum toluene fluxes were observed during the pollutant loading intervals (when air flow rates were highest) while minimum fluxes were observed during toluene non-loading intervals when air flow rates were reduced. Minimum fluxes were not equal to zero even when no toluene was being supplied to the system, as long as at least some air flow was continuously supplied to the system. Toluene, which temporarily accumulated in the GAC during the daily loading intervals, redistributed in the reduced airflow. The redistribution in time when toluene exited the column relative to when it entered resulted in maximum toluene concentrations (Fig. 1) and fluxes (Figs. 4 and 5) exiting the columns that were lower than the influent loading.

In an integrated system comprised of a GAC column followed by a biofilter, this could be used to achieve the practical advantage of decreasing peak contaminant loading rate to the biofilter. If design of a downstream biofilter was based on peak contaminant loading rate as advocated by some authors [20,29,30], a smaller biofilter could be used to remove the VOCs. Alternately, a GAC column could be used to increase pollutant removal efficiency or provide a safety factor in design [20]. Importantly, this approach could also be used to continuously supply substrate to the biofilter (albeit at a lower mass loading rate) to maintain induction of degradative enzymes and minimize starvation of microorganisms in the biofilter. Previous research has demonstrated that supplemental feed at a contaminant mass loading rate equal to a relatively small fraction of that during normal loading (e.g., 12%) could decrease the length of time required for a biofilter to regain high removal efficiency following shut-down periods by as much as 70% [13]. Use of a GAC load equalization device to provide such contaminant feed could avoid two potential disadvantages of providing supplemental contaminant feed to biofilters from an external source. First, it would avoid the additional cost of the supplemental chemical feed-stock, and second, it would avoid the risk of increasing the overall contaminant mass emitted by the facility if the supplement itself was not completely degraded in the biofilter.

In practice, operators of biofilters treating contaminated gas streams sometimes employ air flow rate reductions during pollutant non-loading intervals to minimize electricity costs associated with blower operation while still maintaining aerobic conditions within the biofilter beds. Research reported here demonstrates that GAC columns can achieve effective load equalization even with decreased flow rates during pollutant non-loading intervals. Such an approach is likely to be especially attractive for processes where contaminants are present in the waste gas for a relatively small fraction of the day. The lower the air flow rate during the pollutant non-loading interval and the longer the daily pollutant loading rate, the higher the resulting average effluent toluene concentration and maximum daily mass flux.

5. Conclusions

- Overall, results from this study demonstrated that load equalization can be achieved by GAC columns which receive intermittent toluene loading in combination with intermittent reduction of air flow rates during toluene non-loading intervals. As the reduction of flow rate during the non-loading period increased, the maximum degree of toluene load equalization that can be achieved by GAC columns decreases.
- GAC column performance under conditions studied with intermittently reduced gas flow rates in columns of packed GAC bed depth of 33.3 cm (4.0 s EBCT at full flow) were able to achieve toluene load equalization close to the theoretical maximum calculated based on overall mass balances.

Acknowledgements

This research was funded by the Governor's Biotechnology Initiative of the Louisiana Board of Regents (grant BOR#015). We thank Calgon Carbon Corp. for providing GAC.

Appendix A. Supplementary data

Supplementary data associated with this article can be found, in the online version, at doi:10.1016/j.cej.2009.11.012.

References

[1] J.S. Devinny, M.A. Deshusses, T.S. Webster, Biofiltration for Air Pollution Control, Lewis Publishers, Boca Raton, FL, 1999.
[2] M. Mohseni, D.G. Allen, K.M. Nichols, Biofiltration of α-pinene and its application to the treatment of pulp and paper air emissions, TAPPI J. 81 (1998) 205–211.
[3] J. Marek, J. Paca, A.M. Gerrard, Dynamic responses of biofilters to changes in the operating conditions in the process of removing toluene and xylene from air, Acta Biotechnol. 20 (2000) 17–29.
[4] W.M. Moe, R.L. Irvine, Effect of nitrogen limitation on performance of toluene degrading biofilters, Water Res. 35 (2001) 1407–1414.
[5] J.C. Atoche, W.M. Moe, Treatment of MEK and toluene mixtures in biofilters: effect of operating strategy on performance during transient loading, Biotechnol. Bioeng. 86 (2004) 468–481.
[6] W.M. Moe, C. Li, Comparison of continuous and sequencing batch operated gas-phase biofilters for treatment of MEK, J. Environ. Eng. 130 (2004) 300–314.

[7] C. Seignez, N. Adler, C. Thoeni, M. Stettler, M. Peringer, C. Holliger, Steady-state and transient-state performance of a biotrickling filter treating chlorobenzene-containing waste gas, Appl. Microbiol. Biotechnol. 65 (2004) 33–37.

[8] C. Li, W.M. Moe, Activated carbon load equalization of discontinuously generated acetone and toluene mixtures treated by biofiltration, Environ. Sci. Technol. 39 (2005) 2349–2356.

[9] W.F. Wright, Transient response of vapor-phase biofilters, Chem. Eng. J. 113 (2005) 161–173.

[10] W.F. Wright, E.D. Schroeder, D.P.Y. Chang, Transient response of flow-direction switching vapor-phase biofilters, J. Environ. Eng. 131 (2005) 999–1009.

[11] D. Kim, Z. Cai, G.A. Sorial, H. Shin, K. Knaebel, Integrated treatment scheme of a biofilter preceded by a two-bed cyclic adsorption unit treating dynamic toluene loading, Chem. Eng. J. 130 (2007) 45–52.

[12] F.J. Martin, R.C. Loehr, Effect of periods of non-use on biofilter performance, J. Air Waste Manage. Assoc. 46 (1996) 539–546.

[13] J. Park, K.A. Kinney, Evaluation of slip feed system for vapor-phase bioreactors, J. Environ. Eng. 127 (2001) 979–985.

[14] H.H.J. Cox, M.A. Deshusses, Effect of starvation on the performance and re-acclimation of biotrickling filters for air pollution control, Environ. Sci. Technol. 36 (2002) 3069–3073.

[15] C. Dirk-Faitakis, D.G. Allen, Biofiltration of cyclic air emissions of alpha-pinene at low and high frequencies, J. Air Waste Manage. Assoc. 53 (2003) 1373–1383.

[16] W.M. Moe, B. Qi, Performance of a fungal biofilter treating gas-phase solvent mixtures during intermittent loading, Water Res. 38 (2004) 2258–2267.

[17] B. Qi, W.M. Moe, Performance of low-pH biofilters treating a paint solvent mixture: continuous and intermittent loading, J. Hazard. Mater. 135 (2006) 303–310.

[18] B. Qi, W.M. Moe, K.A. Kinney, Treatment of paint spray booth off-gases in a fungal biofilter, J. Environ. Eng. 131 (2005) 180–189.

[19] F.J. Weber, S. Hartmans, Use of activated carbon as a buffer in biofiltration of waste gases with fluctuating concentrations of toluene, Appl. Microbiol. Biotechnol. 43 (1995) 365–369.

[20] W.M. Moe, C. Li, A design methodology for activated carbon load equalization systems applied to biofilters treating intermittently generated toluene concentrations, Chem. Eng. J. 113 (2005) 175–185.

[21] W.M. Moe, K.L. Collins, J.D. Rhodes, Activated carbon load equalization of gas-phase toluene: effect of cycle length and fraction of time in loading, Environ. Sci. Technol. 41 (2007) 5478–5484.

[22] M.M. Nabatilan, A. Harhad, P.R. Wolenski, W.M. Moe, Activated carbon load equalization of transient concentration spikes of gas-phase toluene, Chem. Eng. J. 152 (2009) 449–457.

[23] J.C. Crittenden, N.J. Hutlzer, D.G. Geyer, Transport of organic compounds with saturated groundwater flow: model development and parameter sensitivity, Water Resour. Res. 22 (1986) 271–284.

[24] D.W. Hand, J.C. Crittenden, D.R. Hokanson, J.L. Bulloch, Predicting the performance of fixed-bed granular activated carbon adsorbers, Water Sci. Technol. 35 (1997) 235–241.

[25] K.A. Mertz, F. Gobin, D.W. Hand, D.R. Hokanson, J.C. Crittenden, Manual: Adsorption Design Software for Windows (AdDesignS^{TM}), Michigan Technological University, Houghton, MI, 1999.

[26] G. Friedman, Mathematical modeling of multicomponent adsorption in batch and fixed-bed reactors, Master Thesis, Michigan Technological University (1984).

[27] L.F. Shampine, M.W. Reichelt, The MATLAB ODE suite, SIAM J. Sci. Comp. 18 (1997) 1–22.

[28] Z. Hashisho, H. Emamipour, M.J. Rood, K.J. Hay, B.J. Kim, D. Thurston, Concomitant adsorption and desorption of organic vapor in dry and humid air streams using microwave and direct electrothermal swing adsorption, Environ. Sci. Technol. 42 (2008) 9317–9322.

[29] R.W. Martin, H.B. Li, J.R. Mihelcic, J.C. Crittenden, D.R. Lueking, C.R. Hatch, P. Ball, Optimization of biofiltration for odor control: model calibration, validation, and applications, Water Environ. Res. 74 (2002) 17–27.

[30] R.W. Martin, J.R. Mihelcic, J.C. Crittenden, Design and performance characterization strategy using modeling for biofiltration control of odorous hydrogen sulfide, J. Air Waste Manage. Assoc. 54 (2004) 834–844.